

A METHODOLOGICAL APPROACH TO THE CHARACTERIZATION OF BRAIN GLIOMAS, BY MEANS OF SEMI-AUTOMATIC MORPHOMETRIC ANALYSIS

ARTUR DAWID SUROWKA^{✉,1}, DARIUSZ ADAMEK², EDYTA RADWANSKA², MAREK LANKOSZ¹, AND MAGDALENA SZCZERBOWSKA-BORUCHOWSKA¹

¹AGH University of Science and Technology, Faculty of Physics and Applied Computer Science, al. A Mickiewicza 30, 30-059 Krakow, Poland; ²Jagiellonian University, Faculty of Medicine, Department of Neuropathology, Chair of Pathomorphology, Krakow, Poland
e-mail: asurowka@agh.edu.pl; mnadamek@cyf-kr.edu.pl; earadwanska@o2.pl; mlankosz@agh.edu.pl; magdalena.boruchowska@fis.agh.edu.pl

(Received July 7, 2013; revised January 1, 2014; revised April 27; accepted May 5, 2014)

ABSTRACT

The aims of this paper were to present a reliable morphometric procedure for glioma analysis for preliminary prognosis and to develop a semi-automatic procedure that is easy to use. The data presented are important to the extent that they verify the reliability of the results by showing that they are consistent with the findings from more complicated automatic analytical tools. The objects for analysis were digital images of haematoxylin-eosin stained glioma samples. The overall analysis consisted of digital image analysis and the determination of morphometric parameters. Interestingly, an increase in the mean values of aspect ratio with increasing malignancy grade was found. Moreover, the morphometric parameters in relation to the histological origin of gliomas were examined and it was found that, the cellular nuclei of glioblastoma multiforme reveal the biggest mean values of aspect ratio compared with other gliomas.

Key words: computer graphics, gliomas, grading, image processing, morphometry

INTRODUCTION

The most widely accepted approach to glioma classification is the scheme recommended by the World Health Organization (WHO). It is a four-grade classification (Louis *et al.*, 2007). Low grade gliomas (grades I, II, such as oligodendroglioma, ependynoma) are well-differentiated, grow slowly, and since they may often be removed by surgery, the prognosis for them is relatively good (Wen and Kesari, 2004; Dymecki and Kulczycki, 2005). On the other hand, high grade gliomas (grade III such as astrocytoma or grade IV, such as glioblastoma) are undifferentiated. They are also anaplastic, fast growing, aggressive, difficult to treat so that they entail a worse prognosis (Schiffer *et al.*, 1983; Dymecki and Kulczycki, 2005).

Routinely, gliomas are recognized thorough an analysis of haematoxylin-eosin (H&E) (Brat *et al.*, 2008) or immunohistochemically stained (*i.e.*, against GFAP factor) brain tissue sections (Dymecki and Kulczycki, 2005). The classification of the glioma tumor is based upon the presence or absence of certain histological features in the population of neoplasma cells (Brat *et al.*, 2008).

In order to provide a precise description of cell properties morphometric methods are now more and more frequently applied. Moreover, “non-conventional” methods such as morphometric analysis, may be used to support routine histopatological diagnoses based on a subjective assessment of them by a histopathologist. The term “morphometry” (or more precisely “histomorphometry”) is a method for the quantitative description of the morphology of histological markers, particularly at cell or nucleus level (Inagawa *et al.*, 2007). Unlike a traditional microscopic histopatological analysis of samples, it allows findings to be numerically expressed (Adamek and Kałuza, 1993) using various planimetric features, such as perimeter, diameter, surface, as well as the level of variability in these features (Nafe and Schlote, 2004).

In order to determine the numerical values of these parameters, the first morphometric measurements were based on the application of measuring tablets (Vilanova *et al.*, 1982), measuring grids (Schiffer *et al.*, 1989), measuring oculars (Martin and Voss, 1982b) along with much manual work. Instead of using tedious manual measurements, as far back as thirty years ago digital image analysis systems were introduced (Martin

et al., 1984a). Now, modern methods for the histo-morphometric examination of brain tumors include methods for digital picture analysis (Nafe *et al.*, 2000a).

The aim of morphometric studies has been to distinguish between some types and grades of gliomas. Such analyses may be valuable due to the significance of the glioma grade in a prognosis. In an effort to find any significant set of morphometric parameters to discriminate between gliomas according to their grades or types, various histological structures have been investigated, including glioma nuclei (Nafe and Schlote, 2002b), glioma vessels (Wesseling *et al.*, 1994) and even nuclear DNA content (Nafe and Schlote, 2005), and the latter is the most frequent subject of analysis. The morphometric evaluation of histological structures is based on an analysis of both planimetric (cross-sectional areas (Nafe *et al.*, 2000a), perimeter, maximum diameter (Nafe *et al.*, 2000a; Nafe and Schlote, 2004) and volumetric parameters, such as nuclear volume density (Adamek and Kałuza, 1993). In order to evaluate more complex properties of cells, shape-related cellular nucleus parameters, such as aspect ratio and the roundness factor are often examined (Leon *et al.*, 1996; Nafe *et al.*, 1999). In turn, more detailed morphometric studies apply Fourier analysis to the outlines of objects/cellular nuclei (*i.e.*, the determination of Fourier amplitudes, which are independent morphometric parameters) (Leon *et al.*, 1996). The most advanced investigations employ methods using topological analysis, such as the determination of mean distances between nuclei or the number of neighboring tumor cells (Kolles *et al.*, 1993). Apart from shape-describing parameters some morphometry-based analyses employ what is known as densitometry analysis to describe nuclear texture parameters (Nafe and Schlote, 2003).

The basis for morphometric analysis are digital images which show the histological sections of tissues (Nafe and Schlote, 2004). Frequently, haematoxylin-eosin staining is used for the purpose of morphometry (Kros *et al.*, 1992). This allows a description of selected features of glioma cellular nuclei, due to the relatively sharp contrast between cell nuclei and surrounding tissue. In order to perform densitometry analysis Fielgen staining (showing the cellular nuclei DNA content) (Cruz-Sánchez *et al.*, 1997) and various kinds of immunohistochemical staining are also applied in neuro-oncological histomorphometric investigations (Ricco *et al.*, 1994; Sallinen *et al.*, 2000).

Morphometric studies are usually supported by simple statistical analysis to determine the mean values of morphometric parameters and their standard deviations (Saito *et al.*, 1994). A few authors have used

more advanced statistical analysis such as statistical tests, *i.e.*, non-parametric Mann-Whitney U test (Nafe and Schneider, 2000b) and discriminant analysis (Glotsos *et al.*, 2008). This approach is necessary to justify the significance of differences noted between analyzed cells/nuclei in relation to their histological properties, using statistical quantitative procedures. With gliomas, such investigations allow a shape-based glioma classification (Nafe and Schlote, 2004). The first investigation using morphological examinations of gliomas for simple and automatic classification was presented by Martin and Voss many years ago. Recently, morphometric-classification studies employ more advanced classification algorithms including algorithmic classifiers (Nafe *et al.*, 2000; Nafe and Schneider, 2000b) and neuronal networks (at present, the most advanced approaches) (Kolles *et al.*, 1995).

Nowadays, "medical" cellular morphometric analysis is closely connected with graphical data analysis. This is because the objects of analysis are stained tissue sections. As an "easy" source of valuable statistical data there are a plethora of morphometric approaches to facilitate the improvement of images. The best example of this is one presented by Landini and Perryer (2009). Their algorithm provides an approach that makes a visual analysis of H&E images possible even for a color-blind person. This also makes further image transformations easier because of a better contrast between a cell and its surroundings. It should be emphasized that similar strategies may make it possible to support (accelerate and improve) modern histopathological methods of medical diagnostics, reducing the number of mistakes during the diagnostic process (Nafe and Schlote, 2004).

Although many glioma classifications have been established, new types are still being reported along with their classification to the suitable malignancy grade. These "sub-groups" vary in their responses to treatment and in their final prognosis (Verhaak *et al.*, 2010). To date, only for glioblastoma multiforme have four putative sub-types been defined as having significant histological features. These are the proneural, neural, mesenchymal, and classical types (Cooper *et al.*, 2010). To meet the need for a robust and efficient morphometric means of distinguishing between them, systems enabling large-scale data processing have recently been designed (Cooper *et al.*, 2010; Verhaak *et al.*, 2010). These systems make it possible to analyze a great variety of morphologic, densitometric and topometric parameters using large-scale data sets (*e.g.*, The Cancer Genome Atlas (TCGA) and the Repository for Molecular Brain Neoplasia Data (REMBRANDT)) (TCGA Consortium, 2008;

Madhavan *et al.*, 2009). Unfortunately, many of these systems are not freely distributed, so there is still a need to develop robust, simple and efficient procedures for image analysis using commonly available software. In an effort to meet these requirements we propose using the ImageJ software, which is freely distributed by the U.S. National Institutes of Health (source: www.rsbl.info.nih.gov/ij) and which makes it possible to perform shape-based morphometric studies of microscopic images.

Our work is aimed at the design of a simple, reproducible and semi-automatic procedure for the morphometric analysis of H&E stained microscopic images. In this paper we explore the possibility of determining simple morphometric properties (e.g. the longest perimeter, diameter, cross-sectional surface area and other aspects) of glioma cell nuclei for several types of gliomas using the easily available software - ImageJ. The analytical details, therefore, presented here have in mind any potential analyst (not always experienced) who would like to perform a preliminary morphometric analysis of brain gliomas. This paper also examines the usefulness of the procedure suggested in terms of accuracy and reproducibility. The results were obtained to verify morphological differences between various types of common gliomas. In order address issues in future glioma classification the parameters of the morphometric study were compared with tumor malignancy grades and their histological origin. The data presented is important to the extent that it justifies the usefulness of the ImageJ software in our morphometric study. The differences between groups were subjected to statistical analysis. The reliability of the results are confirmed by showing that they are consistent with findings from more complicated automatic analytical tools. The differences between the groups analyzed are subjected to statistical analysis. Although several studies have indicated that there exist some differences in the shape and size of cells, little attention has been paid to differences between individual cases. Thus, except from analysis of groups of glial tumors (divided in relation

to tumor grade or type), the authors also suggest a preliminary study of the sources of differences (meaning among parameters and their combinations) between some gliomas.

MATERIALS AND METHODS

SAMPLE DESCRIPTION

Digital morphometric analysis was performed on human autopsy samples stained with haematoxylin-eosin, while 13 histopathological slides were prepared and diagnosed in the Department of Neuropathology, Institute of Neurology, Jagiellonian University, Medical College in Krakow. All microscopic images were exported to the 'tiff' format, conserving both the same resolution (1280×960 which is equivalent to $310.7 \mu\text{m} \times 233.0 \mu\text{m}$) and magnification. Nineteen other cases were drawn from The Cancer Genome Atlas1 (TCGA) project data set (TCGA Consortium, 2008). All images were captured at the same magnification and adjusted to the same resolution as above. In all, thirty two cases of brain gliomas were studied. These comprised nine diagnosed histopatologically as glioblastoma multiforme (GM), seven cases of oligodendroglioma (O), four cases of anaplastic oligodendroglioma (OA), four cases of anaplastic astrocytoma (AA), three cases of diffuse astrocytoma (ADm) and five cases of gemistocytic astrocytoma (AG). A short description of all cases, including symbols representing the sample, histopatological diagnosis, WHO-grade, and the number of analyzed images is presented in Table 1.

DESCRIPTION OF PROCEDURE APPLIED

The morphometric analysis included both image post-processing and a determination of the morphometric properties of cell nuclei. All image transformations and morphometric parameter calculations were carried out using "ImageJ" software (source: www.rsbl.info.nih.gov/ij).

Table 1. *A characterization of all cases analyzed.*

Case ID	Diagnosis	WHO grade	Number of analyzed images
O	Oligodendroglioma	II	24 (7 cases)
OA	Anapl. Oligodendroglioma	III	15 (4 cases)
ADm	Diffuse Astrocytoma	II	13 (3 cases)
AG	Gemistocytic Astrocytoma	II	18 (5 cases)
AA	Anaplastic Astrocytoma	III	15 (4 cases)
GM	Glioblastoma	IV	26 (9 cases)
		Sum (cases)	111(32)

In order to single out the cellular nuclei in each image, a few transformations were carried out. "ImageJ" treats every black grouping as an object so every cell in each image needs to be transformed into black pixel groups on a white background (this is called segmentation). The image transformations were carried out in the following stages:

- Scale-bar calibration;
- Color deconvolution, by means of a "Color deconvolution" plugin (for vectors dedicated to H&E images) (*cf.*, Fig. 1);
- Binarization of analyzed images (with one appropriate threshold);
- Application of "Open" and "Close" morphological transformations;
- A "Fill holes" operation on the cell nuclei surfaces;
- Separation of 'bonded' nuclei (watershed transformation);
- Application of the "Erode" transformation;
- The use of a median filter (radius = 2.0);
- Application of the "Dilate" transformation, by means of "Binary Dilate No Merge 8" plugin (www.rsb.info.nih.gov/ij).

The results of the most important transformations to make an image ready for morphometric analysis are graphically presented in Fig. 1.

Finally, the data was transferred to ROI manager to verify the segmentation quality. This tool facilitates the marking of all analyzed object contours on the original image. This operation allows for the correction of unwanted artifacts (endothelial cells, vessels and other non-glioma components) which occur as a result of image transformations and also facilitates the marking of weakly stained glial tumor cells.

Subsequently, for the quantitative characterization of the geometric properties of glioma cell nuclei the morphometric parameters were determined. The simplest parameters, such as cross-sectional nucleus area (A), perimeter (P) and the longest diameter (D, Feret's diameter) were determined. The more "complex" parameters were also calculated. One of them is circularity (C). This parameter can be determined according to equation (1) (Ferreira and Rosband, 2012).

Circularity describes the degree of similarity of an object to a circle, *i.e.*, for a circular object ($Area = \pi \cdot R^2$ and $Perimeter = 2 \cdot \pi \cdot R$, where R is the length of the radius of the circle) circularity is equal to one,

while when a shape is more elliptical it is less than one.

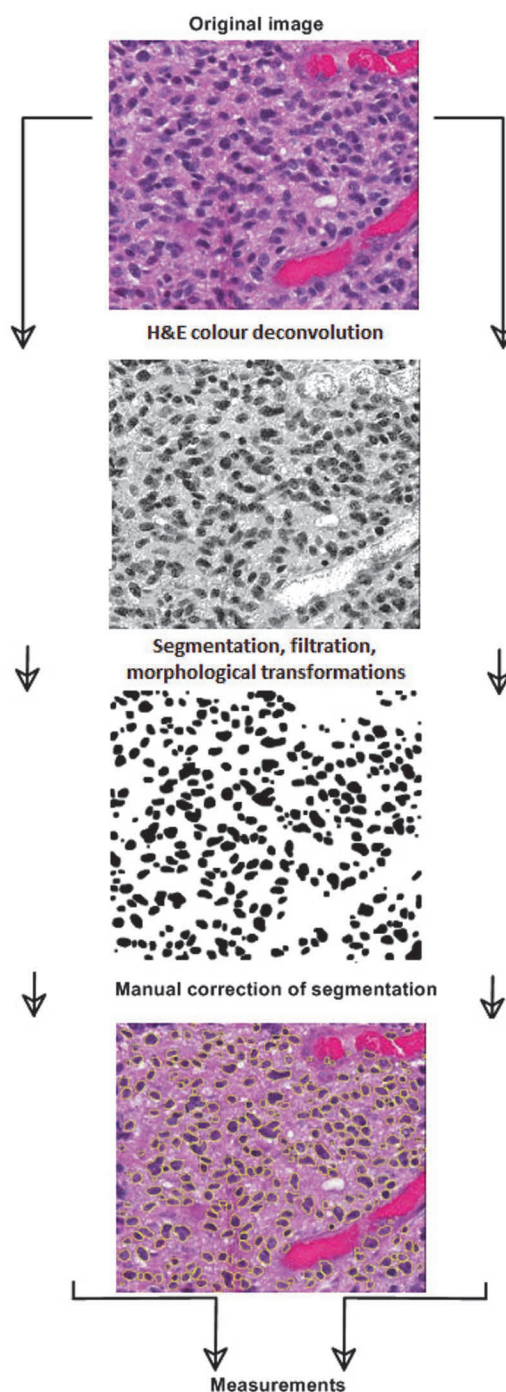


Fig. 1. Stages of segmentation process.

$$C = (4 \cdot \pi \cdot Area) / (Perimeter^2). \quad (1)$$

A further parameter of morphometric analysis is the aspect ratio (AR). This factor was calculated using expression (2) (Ferreira and Rosband, 2012).

$$AR = (a_{max}) / (a_{min}), \quad (2)$$

where: a_{max} – is the length of the major axis of ellipse fitted to an object (μm), a_{min} – is the length of the minor axis of ellipse fitted to an object (μm).

The aspect ratio describes the object's elongation. It is clear that for a circular object ($a_{\max} \approx a_{\min}$) the AR tends to one, but for elliptical objects (non-circular, $a_{\max} > a_{\min}$) the AR is more than one.

The statistical data evaluation was performed using the STATISTICA 10.0 package. Data were analyzed by the method of descriptive statistics. Moreover, a non-parametric Kruskal-Wallis test was applied to the comparison of groups.

VERIFICATION OF APPLIED PROCEDURE

To validate the presented algorithm (*cf.*, Fig. 1), it is crucial to evaluate the suggested procedure in terms of accuracy and reproducibility. For this purpose, two additional evaluations were carried out. All calculations were based on the analysis of 6 small ($100 \mu\text{m} \times 100 \mu\text{m}$) microscopic images (*see* Fig. 9) showing the most representative areas of each analyzed tumor (one image for each kind of glioma). Thus, we started by investigating the values obtained using traditional manual counting/markings. To this end, three independent evaluators, specialized in the field of histopathology, marked – by computer mouse – all outlines of cellular nuclei visible in each image analyzed. Measurements of all manually marked cells were carried out using ImageJ. All non-glial elements, including epithelial cells, were excluded from further analysis. Following the manual measurements, each evaluator calculated the set of the mean values of all morphometric parameters taken into account for each microscopic image analyzed (Fig. 9). Finally, based on these three observations the mean values, along with their unbiased estimations of standard deviation, were calculated for all morphometric parameters. These values were treated as a set of reference parameters. In other words, these measurements gave us the opportunity to evaluate how the mean values of morphometric parameters may vary from one manual measurement to another. Secondly, using the semi-automatic procedure (Fig. 1), each microscopic image was analyzed 10 times. All evaluations included the calculation of representative mean values of ten measurements, together with their unbiased estimators of standard deviation. In turn, these measurements gave us an opportunity to evaluate how the mean values vary from one semi-automatic measurement to another. Thus, based on these ten semi-automatic calculations, reproducibility was calculated for each photo (glioma) and for each morphometric parameter as a ratio of their unbiased sample standard deviation and mean value multiplied by 100%. Finally, the accuracy was calculated for each microscopic image as the percentage

difference between the mean value of a morphometric parameter obtained via manual evaluation (standard value) and the mean value obtained as a result of 10 repetitions (measured value) of a whole semi-automatic procedure.

RESULTS

In this paper, the authors offer a simple and reproducible algorithm for the morphometric analysis of some glial tumors, along with a verification of the procedure and a preliminary analysis of numerical values. For this purpose over 39 000 cell nuclei were measured. The statistical evaluation of data was performed using two criteria of data separation. For the first one, the results of the morphometric description were analyzed in relation to the malignancy grade of brain gliomas according to the latest WHO classification (Louis *et al.*, 2007). Tumors representing the second (II), third (III) and fourth (IV) malignancy grade were studied. The distribution of the measured objects in relation to malignancy grade is presented in Fig. 2. This graph shows that the nuclei of grade IV gliomas constituted the most numerous group and those of grade III gliomas the least. The population of grade II gliomas is somewhere between those of grades III and IV. The second criterion involved the tumor type. In this case the results of the morphometric analysis of brain glioma nuclei were divided into six groups according to histopathological recognition of tumors. The distribution of the cardinality of measured nuclei with respect to histological origin is presented in Fig. 3. This diagram shows that there were the most of GM nuclei analyzed. On the other hand, the smallest population out of the cells analyzed is that of O cellular nuclei.

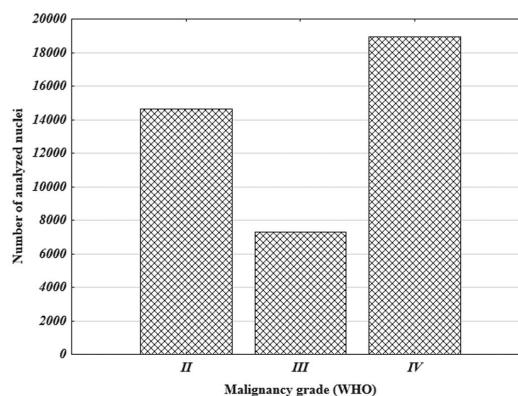


Fig. 2. The distribution of measured cellular nuclei in relation to their malignancy grade.

Using each method of separation for all morphometric parameters, the group mean values, standard

errors of the mean values and the width of confidence interval were calculated. These values are presented

in Figs. 4 and 5, showing tumors of different grades of malignancy and various tumors types, respectively.

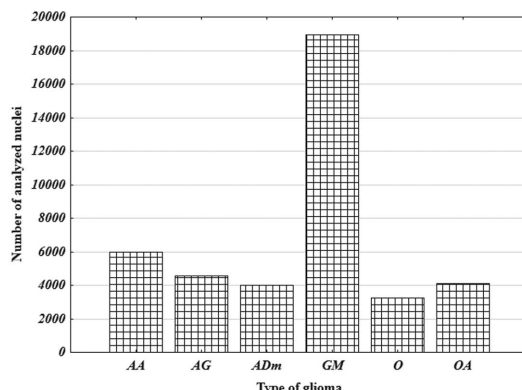


Fig. 3. The distribution of measured cellular nuclei in relation to glioma type.

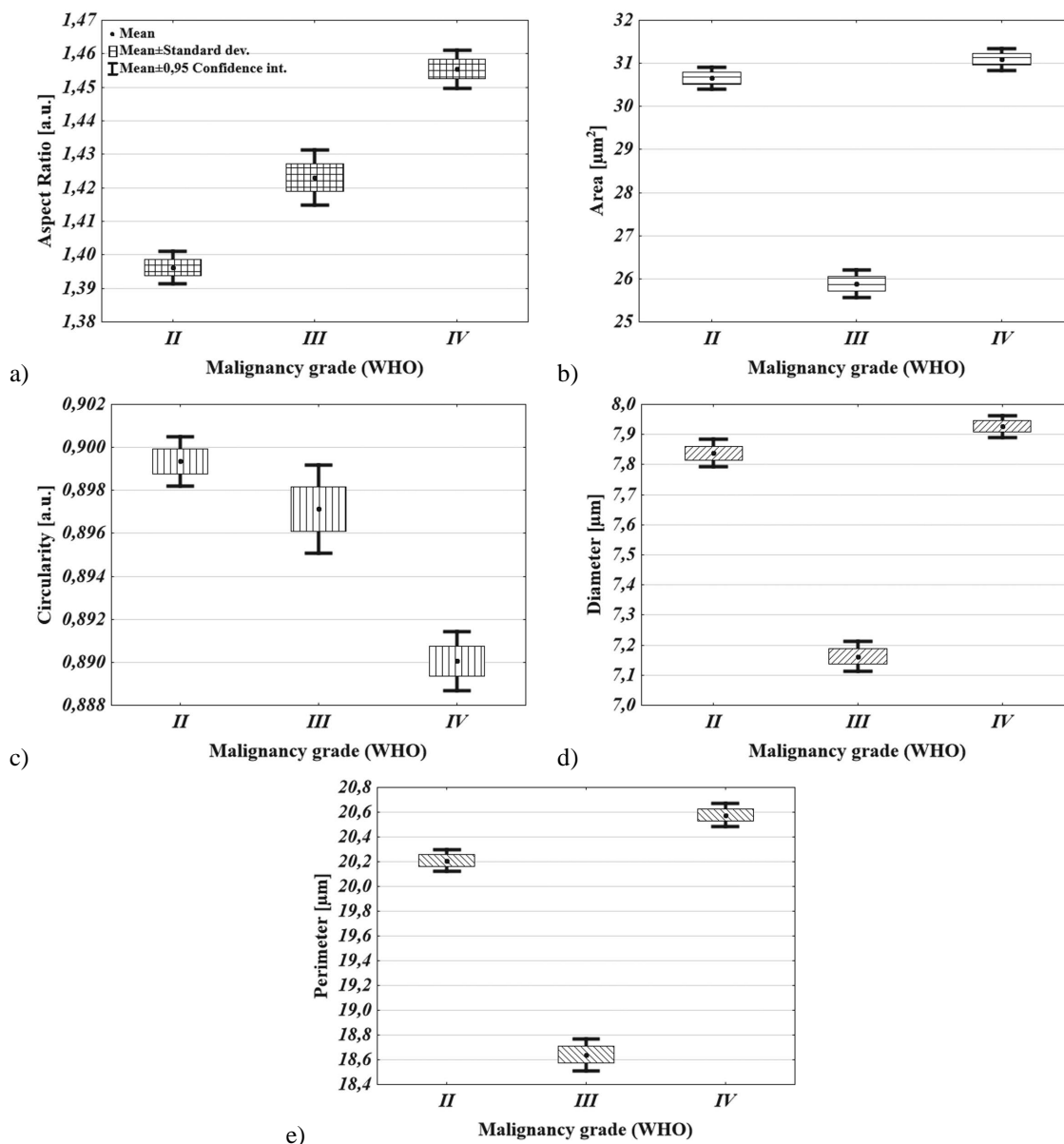


Fig. 4. Comparison of mean values of morphometric parameters in relation to glioma malignancy grade, where: a) aspect ratio b) area c) circularity d) diameter e) perimeter.

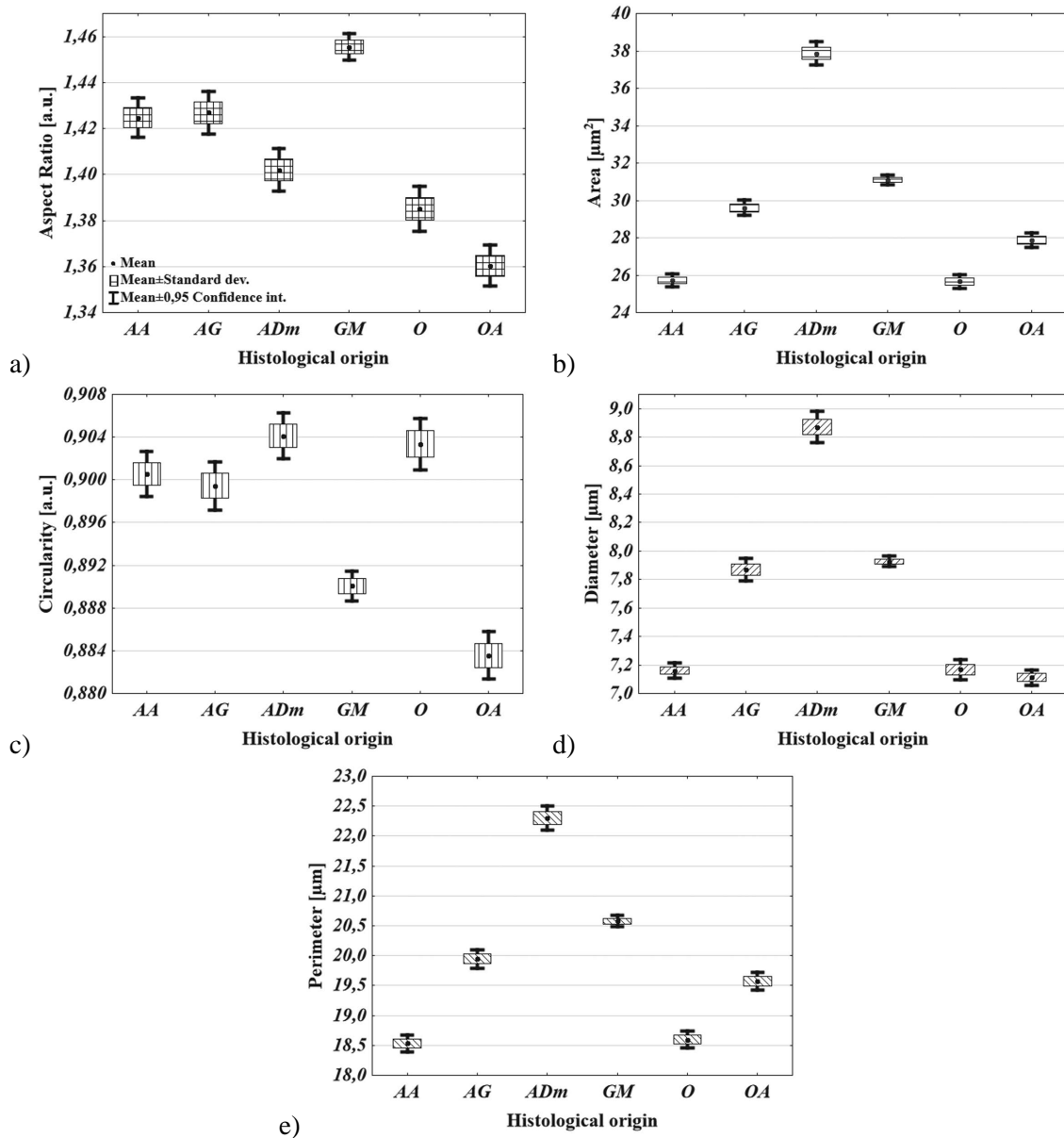


Fig. 5. Comparison of mean values of morphometric parameters with respect to glioma histological origin, where: a) aspect ratio b) area c) circularity d) diameter e) perimeter.

In order to verify the variability of geometric features for a given type of glioma, an individual comparison of morphometric parameters within the given group of gliomas was performed. Such analysis was carried out for seven cases of oligodendroglioma, four cases of anaplastic oligodendroglioma, nine cases of glioblastoma multiforme, five cases of gemistocytic astrocytoma and four cases of anaplastic astrocytoma. Due to the relatively low number of cases, the results for diffuse astrocytoma are presented in Fig. 7 without further statistical analysis. For a visual representation of the mean values of morphometric parameters for all oligodendroglioma tumors (oligodendroglioma and anaplastic oligodendroglioma), astrocytic gliomas

(gemistocytic astrocytoma, diffuse astrocytoma and anaplastic astrocytoma) and glioblastoma multiforme taken into account, the reader is referred to Fig. 6, Fig. 7 and Fig. 8, respectively.

As mentioned above, the differences between the analyzed groups, for each criterion of data separation, and for all analyzed morphometric parameters were verified using the non-parametric Kruskal-Wallis test (H). A non-parametric test was applied because the data set did not fulfill the criteria required for parametric statistical tests. As mentioned above, due to the relatively low number of cases representing diffuse astrocytoma, this group was excluded from deeper

statistical data retrieval. The overall measurement results of the Kruskal-Wallis test are summarized in Tables 2-5. In particular, Tables 2-4 show all parameters for which differences between analyzed cases within a given tumor type were observed. These tables were constructed using the results of the Kruskal-Wallis test for multiple comparisons, meaning that all glioblastoma, oligodendroglioma, etc. cases are compared. All groups of parameters for which statistically

significant differences between given cases were observed, are presented in Tables 2-4; *i.e.*, first row of Table 2 may be interpreted as follows: between O1 and O7 cases only one statistically significant difference in relation to the circularity parameter was observed. On the other hand, for OA cases there were no statistically significant differences in relation to the circularity parameter.

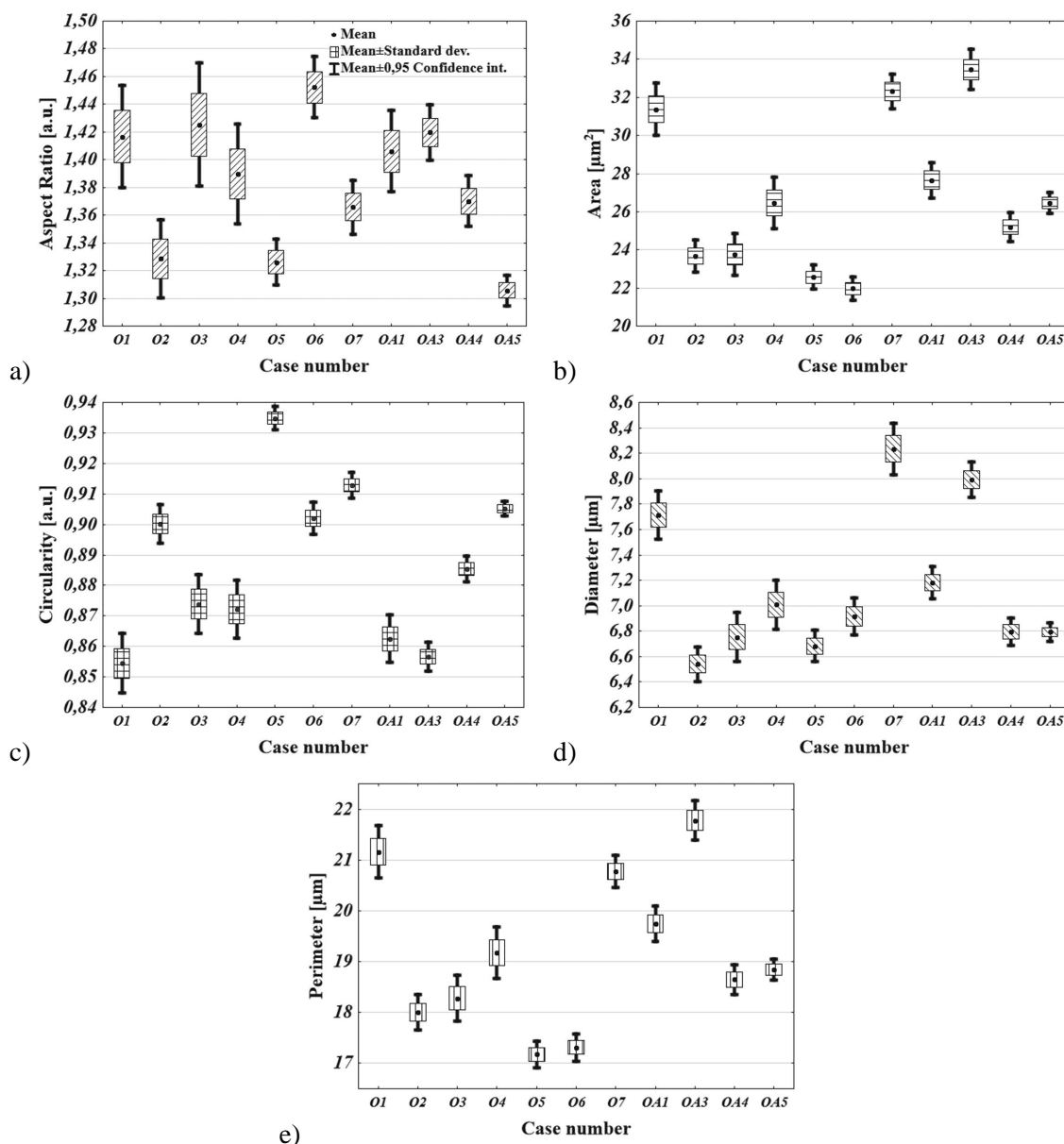


Fig. 6. Comparison of mean values of morphometric parameters between all oligodendroglioma cases, where: a) aspect ratio; b) area c) circularity d) diameter e) perimeter.

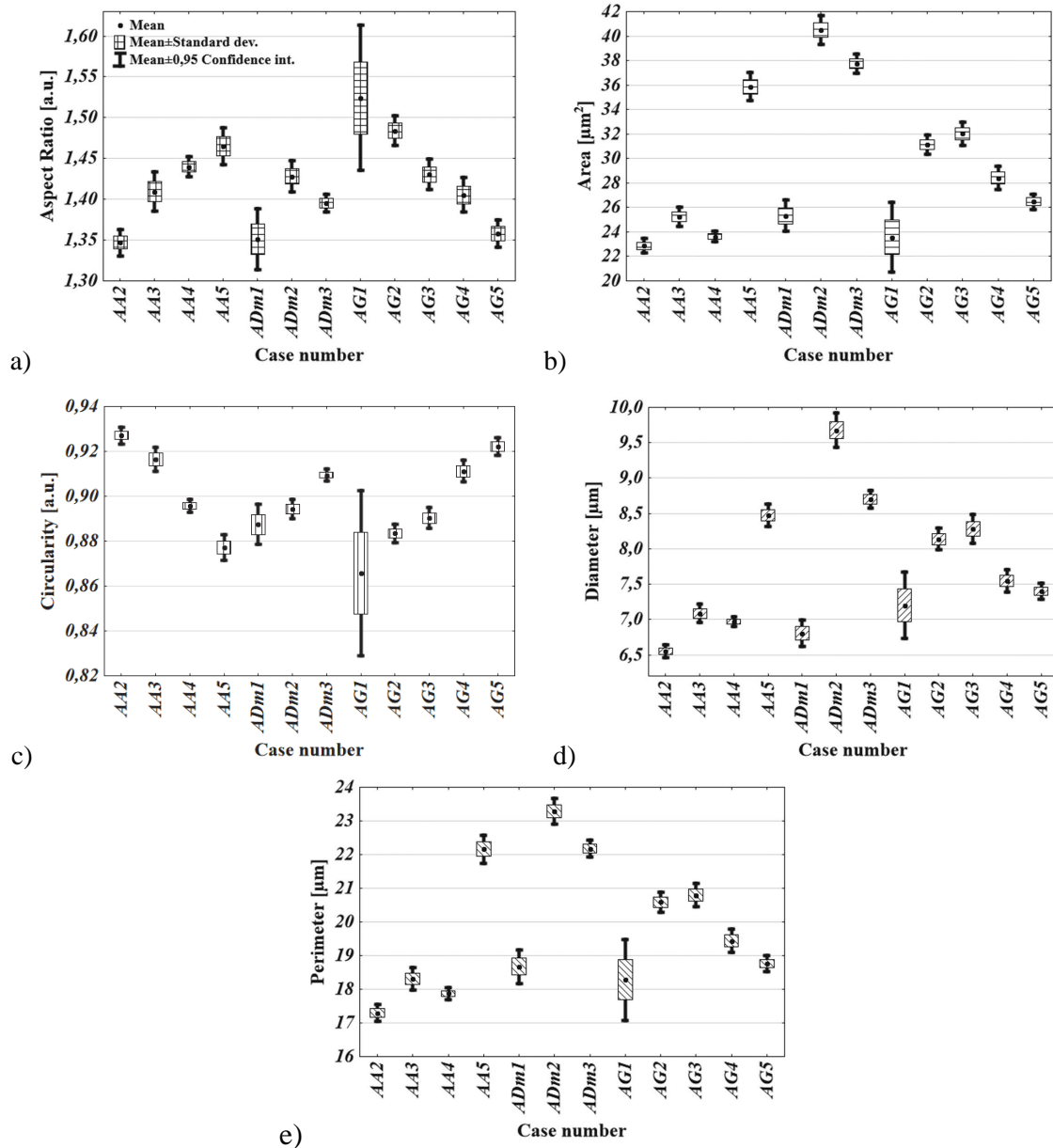


Fig. 7. Comparison of mean values of morphometric parameters between all astrocytic cases, where: a) aspect ratio; b) area c) circularity d) diameter e) perimeter.

The percentage differences relating to each parameter among various glioma types are presented in Table 5. This value was calculated for each tumor type based on the results attached in Tables 2-4, and in particular the ratio of the number of statistically significant differences for a given parameter to the

number of all comparisons for this parameter (between various individuals). Additionally, the mean values of the percentage differences for each glioma type were calculated. The data presented in Table 6 show those morphological parameters for which differences between various tumor types were found.

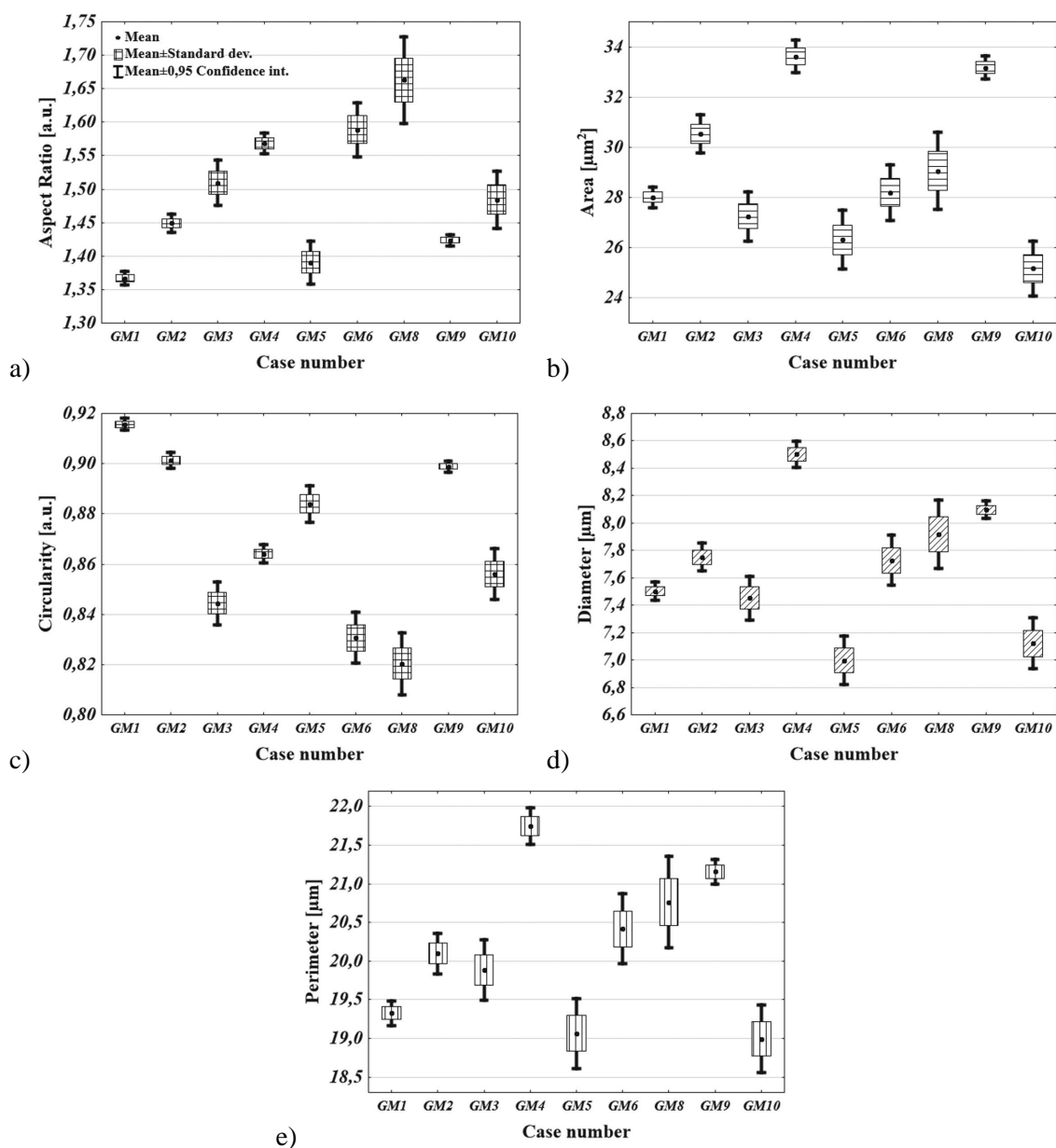


Fig. 8. Comparison of mean values of morphometric parameters between all glioblastoma cases, where: a) aspect ratio; b) area c) circularity d) diameter e) perimeter.

The results of validation procedure including, among others the values of accuracy and reproducibility are

shown in Table 7. In turn, all images used in our verification procedure are presented in Fig. 9.

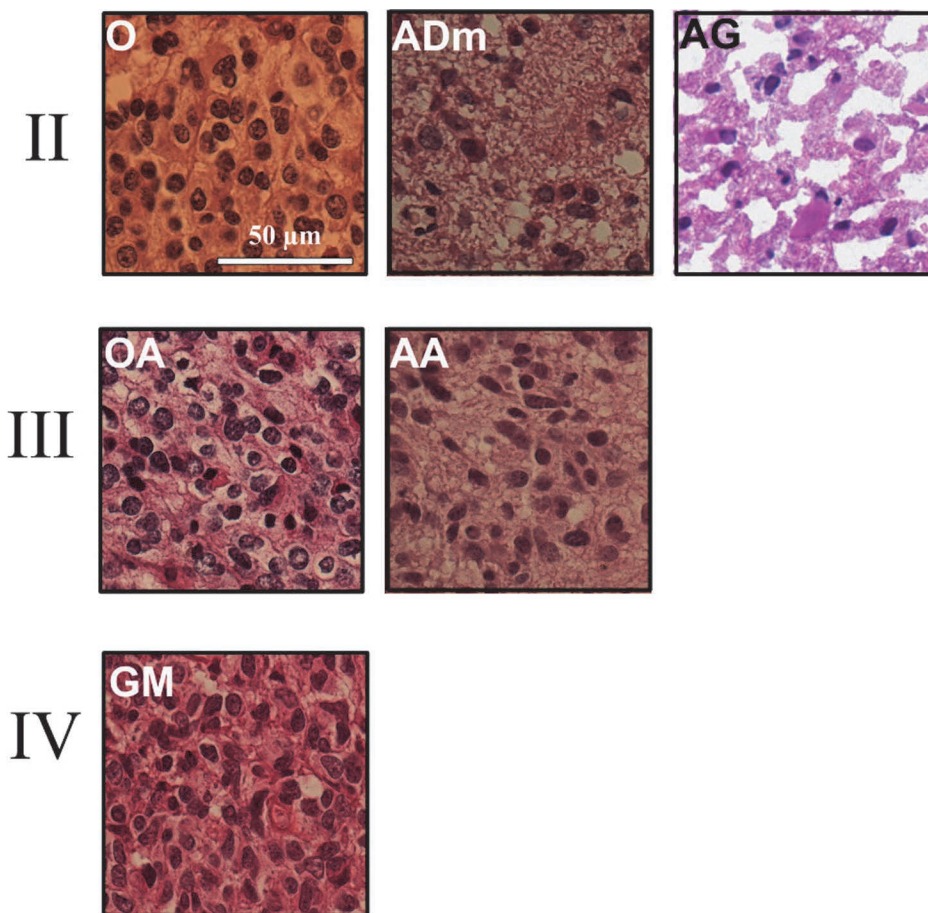


Fig. 9. Set of images used as a validation set. Each image is 100 μm × 100 μm in size.

Table 2. Results of Kruskal-Wallis test. Sets of parameters with differences ($p < 0.05$) between analyzed oligodendroglial cases.

Number of parameters	Parameter(s)	Types of compared oligodendroglomas	
		O	OA
1	C	(1): 1-7;	0**
2	P,C	(2): 2-5; 3-6;	0**
	P,D	(1): 2-4;	0**
3	C, AR	(2): 2-3; 5-6;	0**
	A,P,C	(1): 4-6;	0**
	A, P, D	(1): 1-4;	(1): 4-2;
	A, P, AR	(1): 2-6;	0**
	A, C, AR	0**	(1): 4-5;
4	P, C, AR	(1): 3-5;	0**
	A,P,C,D	(7): 1-3,6;7-2,3; 4-5,7; 5-7	(3): 1-2,4; 3-2;
	A,P,D,AR	(1): 6-7;	0**
5	P,C,D,AR	0**	(1): 1-5;
	ALL	(2): 1-2,5;*	(4): 3-1,4,5; 5-2;*
0	NOT	(1): 3-4;	0**

*The comparisons with differences in relation to all parameters are in bold. **Differences not found.

Table 3. Results of Kruskal-Wallis test. Sets of parameters with differences ($p < 0.05$) between analyzed astrocytic cases.

Number of parameters	Parameter(s)	Type of compared astrocytomas	
		AA	AG
1	A	0**	(1): 1-2;
	AR	0**	(2): 1-4; 2-3;
2	A,P	0**	(1): 1-3;
	C, AR	0**	(2): 1-5; 4-5;
3	C, D, AR	(1): 2-4;	0**
4	A,P,C,D	(1): 4-5;	(1): 3-4;
	A, P, C, AR	(1): 3-4;	0**
	A,P,D,AR	(1): 2-3;	0**
5	ALL	(2): 5-2,3*	(3): 2-4,5; 3-5;*
0	NOT	0**	0**

*The comparisons with differences in relation to all parameters are **in bold**. **Differences not found.

Table 4. Results of Kruskal-Wallis test. Sets of parameters with differences ($p < 0.05$) between analyzed glioblastoma multiforme cases.

Number of parameters	Parameter(s)	GM: Pairs of cases indicating statistically significant differences related to given set of parameters
1	C	(1): 3-10;
2	A,C	(1): 4-8;
	C, D	(3): 1-10; 5-6; 5-10;
	C, AR	(5): 2-6;3-5,6; 4-10; 6-10;
3	A, P, D	(1): 9-10;
	A, C, D	(2): 1-8; 2-10
	A, C, AR	(2): 1-9; 4-9;
	P, C, AR	(2): 1-6; 4-6;
	P, D, AR	(1): 1-2;
	C, D, AR	(2): 1-5; 8-9;
4	A,P,C,D	(4): 2-8,9; 3-8; 5-9;
	A,P,D,AR	(1): 5-8;
	A,C,D,AR	(1): 3-9;
	P,C,D,AR	(2): 2-4; 4-5;
5	ALL	(3): 6-8,9; 8-10;*
0	NOT	(5): 1-3,4; 2-3,5;3-4

*The comparisons with differences in relation to all parameters are in bold.

Table 5. The percentage of differences regarding each parameter among various glioma types.

Type	Area	Per	Circ	Diameter	AR	Mean
O	62	81	81	57	33	63
OA	100*	83	100*	83	67	87*
AG	90*	60	90*	60	90*	78
AA	83	83	83	83	83	83
GM	42	36	78	53	56	53

*The percentages with the most differences (>85%) are **in bold**.

Table 6. Results of Kruskal-Wallis test. Sets of parameters with differences ($p < 0.05$) between analyzed types of gliomas.

Number of parameters	Parameter(s)	Types of gliomas indicating an occurrence of statistically significant differences
1	AR	(1): AA-O;
3	A, P, D	(2): AA-AG; ADm-O;
4	A,P,C,D A,P,D,AR	(4): OA-AA, ADm; AG-OA; O-OA (3): ADm-AA,AG; AG-O; AA-OA
5	ALL	(5): GM-AA, ADm, AG, O, OA* ;
0	NOT	0**

*The comparisons with differences in relation to all parameters are **in bold**. **Differences not found.

Table 7. Comparison of numerical values of morphometric parameters obtained during manual measurements, automatic measurements, together with accuracy and reproducibility parameters.

Type	Number of cells	Area [μm^2]	Perim [μm]	Circ [a.u.]	Feret [μm]	AR [a.u.]
Values calculated by three independent histopathologists						
AA	71 \pm 1	27.9 \pm 0.4	19.8 \pm 0.2	0.87 \pm 0.01	7.5 \pm 0.1	1.52 \pm 0.01
ADm	38 \pm 1	27.3 \pm 0.7	19.4 \pm 0.1	0.88 \pm 0.01	7.29 \pm 0.03	1.48 \pm 0.05
AG	22 \pm 1	19.1 \pm 0.4	16.8 \pm 0.1	0.81 \pm 0.01	6.41 \pm 0.04	1.65 \pm 0.05
GM	97 \pm 3	31.8 \pm 0.6	21.5 \pm 0.2	0.84 \pm 0.01	8.30 \pm 0.04	1.66 \pm 0.02
O	85 \pm 2	30.3 \pm 0.6	20.3 \pm 0.1	0.889 \pm 0.001	7.5 \pm 0.1	1.38 \pm 0.01
OA	83 \pm 1	33.1 \pm 0.9	21.3 \pm 0.3	0.891 \pm 0.001	7.9 \pm 0.1	1.43 \pm 0.03
Values calculated by means of ImageJ*						
AA	72 \pm 1 (1.4%)	27.6 \pm 0.5 (1.1%)	19.7 \pm 0.2 (<1%)	0.874 \pm 0.004 (<1%)	7.4 \pm 0.1 (1.4%)	1.45 \pm 0.02 (4.8%)
ADm	37 \pm 1 (2.7%)	27.6 \pm 0.7 (1.1%)	19.5 \pm 0.3 (<1%)	0.88 \pm 0.01 (<1%)	7.3 \pm 0.1 (<1%)	1.4 \pm 0.2 (4.1%)
AG	21 \pm 1 (<1%)	19.7 \pm 0.4 (3%)	16.7 \pm 0.2 (<1%)	0.84 \pm 0.01 (3,6%)	6.3 \pm 0.1 (1.7%)	1.55 \pm 0.04 (6.1%)
GM	99 \pm 1 (2.1%)	31.8 \pm 0.8 (<1%)	21.4 \pm 0.3 (<1%)	0.84 \pm 0.01 (<1%)	8.1 \pm 0.1 (2.4%)	1.58 \pm 0.02 (4.8%)
O	84 \pm 1 (1.2%)	30.5 \pm 0.6 (<1%)	20.4 \pm 0.3 (<1%)	0.883 \pm 0.003 (<1%)	7.5 \pm 0.1 (<1%)	1.34 \pm 0.01 (2.9%)
OA	84 \pm 1 (1.2%)	32.0 \pm 0.7 (3.3%)	20.9 \pm 0.3 (1.9%)	0.892 \pm 0.003 (<1%)	7.5 \pm 0.1 (5.1%)	1.33 \pm 0.02 (3.5%)
Reproducibility [%]						
AA	99.0	98.3	99.1	99.6	98.9	98.9
ADm	97.7	97.4	98.6	99.3	98.5	98.8
AG	97.9	98.2	98.9	98.3	98.9	97.4
GM	99.3	97.5	98.7	99.3	98.5	99.7
O	99.0	97.7	98.8	99.6	98.9	99.2
OA	99.3	97.9	98.7	99.6	98.5	98.3

*Value in parenthesis represents the percentage difference between the mean value of a given parameter by means of presented algorithm and manual marking.

DISCUSSION

As shown in Fig. 9 oligodendroglioma cells exhibit the most circular shape compared with other gliomas (Engelhard *et al.*, 2002). This is a natural consequence of the histological origin of this tumor, which shares the most common histological properties with oligodendrioma cells (Engelhard *et al.*, 2002). This observation is justified by our morphometric analysis. We found that oligodendrioma tumors show the lowest value of aspect ratio (the tendency towards a regular-circular shape, *cf.*, Fig. 5). Moreover the data presented in Fig. 6 and in Table 5 suggest that this group is relatively the most homogenous regarding aspect ratio (AR). It was also observed that two individuals with pure oligodendroglioma (*i.e.*, O1 and O7) exhibit

many statistically significant differences in relation to most morphometric parameters, including perimeter, diameter and area (Table 2). This suggests that in the cellular nuclei of individual glioma cases, there can be radical changes of shape and size. Furthermore, it can be seen that they indicate the highest mean values of these parameters compared with other oligodendroglioma cases (*cf.*, Fig. 6). However, most cases are rather homogenous in relation to all the morphometric parameters analyzed. Interestingly, there are also statistically significant differences between two major oligodendroglioma types, those being oligodendroglioma and its anaplastic form – anaplastic oligodendroglioma (higher grade III, *cf.* Table 6). As follows from Table 6, there are in these types of gliomas many statistically significant differences in relation to

the parameters of area, perimeter, circularity and diameter. This observation implies that the anaplasia of oligodendrioma cells may affect the elongation, shape and size of the nucleus. In particular, cellular nuclei belonging to OA exhibit the biggest mean values of area and perimeter compared with O (see Figs. 5, 9 and Table 6). The mean value of area for O is $26 \mu\text{m}^2$, while for OA it is $28 \mu\text{m}^2$. Furthermore, the mean value of circularity (C) is 0.903 for O and about 0.884 for OA showing that the increase in the malignancy grade of oligodendroglioma tumors coincides with distinct changes in the shape of nuclei (cf., Fig. 9). All the results mentioned above are consistent with other morphometric studies which contain comparable observations (i.e., Nafe *et al.*, 1999). Furthermore, for OA individuals we observed the most individual differences for all morphometric parameters (cf., Table 5). More precisely, these cells may exhibit the most individual differences in relation to area, circularity and diameter compared with other types. This suggests that the anaplasia of oligodendrioma tumors may affect the homogeneity of both cell shape and size.

Astrocytic tumors were also featured in our study. As follows from Fig. 9 the cell nuclei of astrocytic tumors are more elongated and non-circular than those of oligodendrioma tumors (Dymecki and Kulczycki 2005; Cooper *et al.*, 2010). Three types of astrocytic tumors were analyzed - anaplastic astrocytoma (AA, grade III), gemistocytic astrocytoma (AG, grade II) and diffuse astrocytoma (ADm, grade II). Based on the results of the Kruskal-Wallis test (cf., Table 6, Fig. 5), we found that the AG and ADm astrocytoma cells have statistically significant bigger mean values of area, perimeter and diameter compared with pure oligodendroglioma (O) cases. In other words, all astrocytoma nuclei reveal significant changes in shape compared with those of oligodendroglioma. Moreover, AG, ADm and AA (especially AA) show higher mean values of AR compared with all oligodendrogliomas (oligoendrogliomas are less elongated – see Fig. 9) analyzed. It was also observed that the mean values of the circularity parameter are usually lower for AG and AA than for oligodendrioma (O) cases (see Fig. 5). In other words, these astrocytic cells are more non-circular than pure oligodendrioma (O) ones. These findings are consistent with previous histopathological observations (Dymecki and Kulczycki 2005; Cooper *et al.*, 2010) and with other morphometric studies of this family of neoplasmas, providing further confirmation of the good quality of the results obtained (Nafe *et al.*, 2000; Sallinen *et al.*, 2000). It is interesting that astrocytoma tumors show an increase

in AR with increasing malignancy grade (from II-nd [i.e., ADm] to III-rd [i.e. AA] grade). These are similar to the findings of Ricco, *et al.* (Ricco *et al.*, 1994). As can be seen in Fig. 5, all astrocytic tumors show a decrease in area and circularity as the malignancy grade of tumors belonging to this family increases (i.e., grade III AA have the lowest mean area values, while grade II ADm has the highest). These observations are not in conflict with other studies of this family of neoplasmas because parallel results were reported by (Nafe and Schlote, 2004b). However, these authors presented only a comparison of area and roundness (the roundness factor being analogous to the concept of circularity used in our work). Nevertheless, they found that the area mean values of all grade II astrocytomas are higher than the values obtained for AA, and this is consistent with our study. It should be mentioned that all AA and AG cases show some statistically significant differences among individual members of these groups (see Fig. 7, Table 3). This may highlight individual variations in the shape and size of these nuclei. As can be seen in Table 5 astrocytic tumors overall show the most individual differences in relation to aspect ratio (see Table 3), which would be the source of individual variation in cell elongation. However, it is very difficult to find analogous observations in the literature because most authors usually analyze glial tumors using large scale data sets, without comparing individual cases.

According to histological observations glioblastoma is the most distinctive brain glioma (Van den Bent, 2008). As shown in Fig. 9, its cells are bigger, and more elongated compared with other gliomas (Kong *et al.*, 2011). It can be seen that our morphometric study provided similar observations as well. From Fig. 3 it is obvious that many more cases had to be analyzed, because of the level of internal cell variability. As can be seen from Table 4 and Fig. 8 both statistical data analysis and a visual evaluation of the mean values of differences of morphometric parameters imply that GM constitutes a family of neoplasmas within which there are some significant differences. These observations highlight the histological variability of these cells, as suggested in other work (Nafe and Schlote, 2004). As regards morphologic properties we observed that GM shows the highest mean values of aspect ratio, which implies that these tumors have the most elongated nuclei (cf. Fig. 5). Interestingly, we noticed that OA cells are much smaller and less circular than GM (Fig. 5). This observation on circularity is not common in other histology-related works in the literature (Nafe and Schlote, 2004). This

may be explained by certain properties peculiar to the particular OA cases used in this study.

It is also worth noting that recent studies show that glioblastoma seems to be the most problematic from a morphometric point of view (Cooper *et al.*, 2010). Firstly, an overlap with data coming from other tumors is observed (Nafe and Schlote, 2004). Secondly, as mentioned above (*see* Introduction), recent studies (carried out on the TCGA data set) show that there may be four clinically significant “sub-families” of glioblastoma, namely proneuronal, neuronal, mesenchymal and classical (Verhaak *et al.*, 2010). The classification issue thus raised is based on an analysis of genomic abnormalities observed among GM affected individuals. This information is highly valuable because these types might vary in relation to severity and stage (Cooper *et al.*, 2010), suggesting some variation in the individual properties of cellular nuclei. Right now, there is much evidence which gives an insight into the morphometric classification of these sub-types (Cooper *et al.*, 2010). However, one must be careful when positing subgroups and analyzing the properties of big groups of glioblastoma multiforme cases in terms of average values alone. It is clear that one of the main challenges for modern morphometric studies is to overcome problems with the correct classification of glioblastomas (Cooper *et al.*, 2010; Kong *et al.*, 2011). These classification issues hinder morphometric studies of glioblastomas, because it might prove difficult to determine the representative mean value of a parameter for an apparent single group (GM), when it may actually split into several “sub-groups”.

Based on the analysis of Fig. 4 and the results of the Kruskal-Wallis test, it was noticed that mean values of all morphometric parameters, calculated separately for each glioma grade (II, III, IV) indicate that there are statistically significant differences relevant to all parameters. Interestingly, the mean values of the AR and C parameters exhibit an interesting association with the level of glioma grade; that is, AR increases the higher the grade, while C decreases (*cf.*, Fig. 4). This suggests that the most malignant gliomas are more elongated and less circular than those of the second and third grades. It is clear that this observation is a natural consequence of gliomas belonging to families of certain grades, *viz.* the most circular oligodendrogliomas (grade II) and the most elongated glioblastomas (grade IV). For a visual representation of the interdependence of aspect ratio with malignancy grade the reader is also referred to Fig. 9, where this is partially visible. It is also worth noting that although these results do not provide any new

insight on the properties of brain gliomas to the best of our knowledge, there is no contribution in the literature which has analyzed and presented morphometric findings which show a similar relationship.

As shown in Fig. 4, since both an increase in the aspect ratio and a decrease in circularity coincided with increasing malignancy grade, it seems possible that these results are due to type of glioma in each grade in this specific study. In particular, as shown in Fig. 9, one can notice that OA and AA cases represent malignant grade III. However, as presented in Fig. 4, these types of gliomas have generally lower mean values of area, diameter and perimeter compared to the other glioma subtypes. This remark, therefore, suggests that area, perimeter and diameter are less useful measures for distinguishing malignancy grade than the aspect ratio and circularity (Fig. 4). In short, this overall conclusion is consistent with other findings found in the literature, suggesting that our procedure produced results which corroborate of a great deal of the previous work in this field (Nafe and Schlote, 2004).

To illustrate the quality of the algorithm presented, an analysis of accuracy and reproducibility factors was performed. Based on the results presented in Table 7, one may conclude that the percentage difference (here, accuracy) between the mean values of morphometric parameters obtained via manual and automatic counting did not exceed 5%, except for the AR parameter in the case of ADm (6% difference, Table 7). This anomaly may be due to the fact that these cells have an irregular shape, together with the occurrence of lightly stained artifacts/nuclei. This may also generate many problems for the appropriate classification of an object as an actual nucleus, both for the manual practitioner and the computer. However, the method here outlined may be an effective way to improve manual morphometric measurements of glial nuclei, because these differences uncovered are usually robust. As can be seen from Table 7, the AR parameter indicates the lowest relative accuracy. This fact might be the result of errors arising from evaluation of minor and major axes (a_{\min} , *see* Eq. 2) and from the calculation of their ratio. As regards reproducibility, the mean values of such parameter did not usually exceed 5%, and the calculations of circularity were of the best quality. On the other hand, the evaluations of area exhibit the lowest, but still adequate reproducibility. The latter may be due to small variations in the manual binarization of analyzed images. To overcome this problem, it is necessary to adopt an automatic (adaptive) alternative for the binarization needed in our procedure.

CONCLUSIONS

The results of our work show that the semi-automatic algorithm presented is completely applicable to the morphometric analysis of images of haematoxylin-eosin stained tissue sections. It should be mentioned that for gliomas indicating relatively high cell density some problems with cell segmentation and separation may occur. In such cases cells were therefore (eventually) manually marked. Thus, the results of the statistical analysis of the data suggest the presence of statistically significant differences between particular glioma grades of malignancy and tumor types in relation to some simple morphometric parameters. For example, the mean value of the aspect ratio increases with increasing malignancy grade and the cellular nuclei of glioblastoma multiforme have the biggest mean values of aspect ratio compared to the other gliomas. These results could be applied to morphometry-based glioma differentiation and diagnostic neuro-oncology.

In our study we designed, applied and verified a methodological approach that may be applied as a method for the quantitative description of brain gliomas. We would emphasize that we presented the approach for the purpose of morphological analysis, rather than to perform a complete morphometric study as such. We would hope that this work can be used as an instruction tool for those who need to do any morphometric analysis of brain gliomas.

ACKNOWLEDGMENTS

This work was supported by the Polish Ministry of Science and Higher Education and its grants for Scientific Research (N N518 377537). This project was prepared with support of "ImageJ" software, freely distributed by the U.S. National Institute of Health. The authors' thanks are due to the TCGA consortium for kindly granting permission to include data drawn from its database (The Cancer Genome Atlas (TCGA) publications policy, source: <http://cancergenome.nih.gov/abouttcga/policies/publicationguidelines>).

REFERENCES

- Adamek D, Kaluza J (1993). Stereological aspects of pathology of gliomas: volume density of nuclei and volume corrected mitotic index. *Acta Stereol* 12:65–70.
- Bjornhagen V, Lindholm J, Auer G (1997). Analysis of nuclear DNA and morphometry and proliferating cell nuclear antigen in primary and metastatic malignant melanoma. *Scand J Plast Reconstr Surg Hand Surg* 31: 109–18.
- Brat DJ, Prayson RA, Ryken TC, Olson JJ (2008). Diagnosis of malignant glioma: role of neuropathology. *J Neuro-oncol* 89:287–311.
- Cooper AD, Kong J, Gutman DA, Wang F, Choleti SR, Pan TC, *et al.* (2010) An integrative approach for in silico glioma research. *IEEE Trans Biomed Eng* 57: 2617–21. doi:10.1109/TBME.2010.2060338
- Daumas-Duport C, Varlet P, Tucker ML, Beuvon F, Cervera P, Chodkiewicz JP (1988a). Grading of astrocytomas. A simple and reproducible method. *Cancer* 62:2152–65.
- Daumas-Duport D, Scheithauer B, O'Fallon J, Kelly P (1988b). Grading of astrocytomas. Simple and reproducible method. *Cancer* 62:2152–65.
- Decaestecker C, Camby I, Nagy N, Brotchi J, Kiss R, Salmon I (1998). Improving morphology-based malignancy grading schemes in astrocytic tumors by means of computer-assisted techniques. *Brain Pathol* 8:29–38
- Dymecki J, Kulczycki J. *Neuropatologia*. Urban & Partner, Wrocław 2005.
- Engelhard HH, Stelea A, Cochran EJ (2002). Oligodendroglioma: pathology and molecular biology. *Surg Neurol* 58:111–7.
- Ferreira T, Rosband W (2012). ImageJ user guide. IJ 1.46r. source: www.rsbl.info.nih.gov/ij/gocs/guide/user-guide.pdf.
- Glotsos D, Kalatzis I, Spyridonos P, Kostopoulos S, Daskalkis A, Anthanasiadis E, *et al.* (2008) Improving accuracy in astrocytomas grading by integrating a robust least squares mapping driven support vector machine classifier into a two level grade classification scheme. *Comput Methods and Progr in Biomed* 90: 251–61
- Gonzales MF (2004). Grading of gliomas. *J Clin Neurosci* 4:16–8.
- Inagawa H, Ischizawa K, Hirose T (2007). Qualitative and quantitative analysis of cytologic assessment of astrocytoma, oligodendroglioma and oligoastrocytoma. *Acta Cytol* 51:900–6.
- Kolles H, Foerderer W, Bock R, Feiden W (1993). Combined Ki-67 and Feulgen stain for morphometric determination of the Ki-67 labelling index. *Histochemistry*. 100:293–6
- Kolles H, Von Wangenheim A, Vince GH, Niedermayer I, Feiden W (1995). Automated grading of astrocytomas based on histomorphometric analysis of Ki-67 and Feulgen stained paraffin sections. Classification results of neuronal networks and discriminant analysis. *Anal Cell Pathol* 8:101–16
- Kong J, Cooper L, Moreno C, Wang F, Kurc T, Saltz J, *et al.* (2011). In silico analysis of nuclei in glioblastoma using large-scale microscopy images improves prediction of treatment response. *Conf Proc IEEE Eng Med Biol Soc* 2011:87–90. doi:10.1109/IEMBS.2011.6089903

- Kros JM, Van Eden CG, Vissers CJ, Muldner AH, Van der Kwast TH (1992). Prognostic relevance of DNA flow cytometry in oligodendroglioma. *Cancer* 69: 1791–8.
- Landini G (2006). Quantitative analysis of the epithelial lining architecture in radicular cysts and odontogenic keratocysts. *Head Face Med* 2006: 2–4. doi: 10.1186/1746-160X-2-4
- Landini G, Perryer GJ (2009). Digital enhancement of haematoxylin- and eosin-stained histological images for red-green color-blind observers. *Microsc* 234:293–301. doi: 10.1111/j.1365-2818.2009.03174.x.
- Leon SP, Folklerth RD, Black PM (1996). Microvessel density is a prognostic factor for patients with astroglial tumors. *Cancer* 77:362–72.
- Louis DN, Ohgaki H, Wiestler OD, Cavenee WK, (eds) (2007). WHO classification of tumours of the central nervous system. IARC, Lyon.
- Madhavan S, Zenklusen JC, Kotilarov Y, Sahni H, Fine HA, Buetow K (2009). Rembrandt: Helping personalized medicine become a reality through integrative translational research. *Mol. Cancer Res* 2:157–67.
- Martin H, Voss K (1982a). Automated image analysis of glioblastomas and other gliomas. *Acta neuropathol (Berl)* 58:9–16.
- Martin H, Voss K (1982b). Computerized classification of gliomas by automated microscope picture analysis. *Acta Neuropathol (Berl)* 58:261–8.
- Martin H, Voss K (1982c). Computerized classification of gliomas by automated microscope picture analysis (AMPA). *Acta Neuropathol (Berl)* 58:261–8.
- Martin H, Voss K, Hufnagl P, Froehlich K (1984a). Automated image analysis of gliomas. An objective and reproducible method for tumor grading. *Acta Neuropathol (Berl)* 63:190–9.
- Martin H, Guski M, Guski H (1984b). Karyometric investigations of meningiomas. *Zentralbl Neurochir.* 45:289–98.
- Nafe R, Schlote W, Schneider B (1999). Quantitative evaluation of nuclear pleomorphism in oligodendroglial tumors by means of Fourier-analysis of nuclear outlines. *Electron J Pathol* 5:994–07.
- Nafe R, Schlote W, Schneider B (2000a). Shape analysis of tumor cell nuclei in ependymomas by means of Fourier analysis. *Anal Quant Cytol Histol* 22:475–82.
- Nafe R, Schneider B (2000b). Data analysis for comparative histometry in pathology- I. Classification procedures and other statistical methods. *Electron J Pathol* 6:3.
- Nafe R, Schlote W (2002b). Methods for shape analysis of two dimensional closed contours – a biologically important but widely neglected field in histopathology. *Electron J Pathol* 8:2.
- Nafe R, Schlote W (2002a). Densitometric Analysis of Tumor Cell Nuclei in low-grade and high-grade Astrocytomas. *Electron J Pathol Histol* 8:2.
- Nafe R, Schlote W (2003). Topometric analysis of diffuse astrocytoma. *Anal Quant Cytol Histol* 25:12–8.
- Nafe R, Schlote W (2004). Histomorphometry of brain tumors. *Neuropathol and Appl Neurobiol* 30:315–28.
- Nafe R, Schlote W, Schneider B (2005). Histomorphometry of tumor cell nuclei in astrocytomas using shape analysis, densitometry and topometric analysis. *Neuropathol Appl Neurobiol* 31:34–44.
- NIH ImageJ software, source: www.rsb.info.nih.gov/ij
- Ohgaki H, Kleihues P (2005). Epidemiology and etiology of gliomas. *Acta Neuropathol* 109: 93–108.
- Prodanov D, Nagelkerke N, Marani EJ (2007). Spatial clustering analysis in neuroanatomy: applications of different approaches to motor nerve fiber distribution. *Neurosci Methods* 160:93–108.
- Ricco R, Serio G, Caniglia DM, Cimmino A, Lettini T, Lozupone A, *et al.* (1994). Size and shape evaluation of astrocytoma nuclei with the shape analytical morphometry software system. *Anal Quant Cytol Histol* 16: 345–50.
- Sallinen SL, Helen PT, Rantala IS, Rautiainen E, Helin HJ, *et al.* (2000). Grading of diffusely infiltrating astrocytomas by quantitative histopathology, cell proliferation and image cytometric DNA analysis. *Neuropathol Appl Neurobiol* 26:319–31
- Saito A, Yoshii Y, Nose T (1994). Image Analysis of nuclear DNA content and morphometric characteristics of the tumor cells in human astrocytomas. *Brain Tumor Pathol* 11:143–6.
- Schiffer D, Giordana MT, Mauro A, Migheli A (1983). Glial fibrillary acid protein (GFAP) in human cerebral tumors. An immunohistochemical study. *Tumori* 69: 95–104.
- Schiffer D, Chio A, Giordana MT, Mauro A, Migheli A, Vigliant MC (1989). The vascular response to tumor infiltration in malignant gliomas. Morphometric and reconstruction study. *Acta Neuropathol* 77:369–78.
- TCGA Consortium (2008). Comprehensive genomic characterization defines human glioblastoma genes and core pathways. *Nature* 455:1061–8.
- The Cancer Genome Atlas (TCGA) publications policy, source: <http://cancergenome.nih.gov/abouttcga/policies/publicationguidelines>
- Ullen H, Falkmer UG, Collins VP, Auer GU (1991). Methodologic aspects of nuclear DNA assessment of gliomas with astrocytic and/or oligodendrocytic differentiation. *Anal Quant Cytol Histol* 13:168–76
- Watkins S, Sontheimer H (2012). Unique biology of gliomas: challenges and opportunities. *Trends in Neurosci* 35, no. 9.
- Wen PY, Kesari S (2004). Malignant gliomas. *Curr Neurol Neurosci Rep* 4:218–27.
- Wesseling P, van der Laak JA, de Leeuw H, Ruiters DJ, Burger PC (1994). Quantitative immunohistological analysis of the microvasculature in untreated human

- glioblastoma multiforme. Computer-assisted image analysis of whole tumor or sections. *J Neurosurg* 81: 902–9.
- Van den Bent MJ, Reni M, Gatta G, Vecht C (2008). Oligodendroglioma. *Crit Rev Oncol/Hematol* 66:262–272.
- Verhaak RGW, Hoadley KA, Purdom E, Wang V, Qi Y, *et al.* (2010). The cancer genome atlas research network. Integrated genomic analysis identifies clinically relevant subtypes of glioblastoma characterized by abnormalities in PDGFRA, IDH1, EGFR, and NF1. *Cancer Cell* 1: 98–110
- Vilanova JR, Burgos-Bretones J, Simon R, Aguirre-Urizar JM, Rivera-Pomar JM (1982). Hypothetical evolution of necrosis in glioblastomas. *Pathol Res Pract* 173:283–93